J. Astrophys. Astr. (1980) 1, 3–16

Comoving Frame Calculations of Spectral Lines formed in Rapidly Expanding Media with the Partial Frequency Redistribution Function for Zero Natural Line Width

A. Peraiah *Indian Institute of Astrophysics, Bangalore* 560034

Received 1980 February 8; accepted 1980 April 7

Abstract. Comoving frame calculations have been used to compute the spectral lines formed in rapidly expanding spherical media. We have employed the angle-averaged partial frequency redistribution function R_I with a two-level atom model in non-LTE atom approximation. A linear velocity law increasing with radius has been employed with maximum velocity at $\tau=0$ being set equal to 30 mean thermal units. It is found that one obtains almost symmetric emission line profiles at large velocities similar to those found in quasars.

Key words: radiative transfer—partial redistribution function—comoving frame—spectral lines

1. Introduction

Many stars (such as early type supergiants, Wolf-Rayet stars etc.), quasars and nuclei of Seyfert galaxies show evidence of mass motion in their outer layers. Calculation of spectral lines formed in such media is extremely complicated because of (i) photon redistribution in the line which is again complicated (ii) by the radial mass motion in the medium.

One must calculate accurately the effect of the latter on the former. The calculations become quite involved simply because photons can be redistributed from any given point to any other point in the interval $\nu_0\,(1-V_{\max}/c)$ to $\nu_0\,(1+V_{\max}/c)$ where ν_0 is the central frequency of the line and $V_{\max}$ is the maximum gas velocity. In the atmospheres of many OB type stars, the gas velocities may be as large as 2000-3000 km s^{-1}, which would be about 100 times the mean thermal unit. If one intends to simulate profiles formed in such media, one has to consider the bandwidth as large as 200 mean thermal units. Recently Hummer and Kunasz (1974), Peraiah (1978), Peraiah and Wehrse (1978) and Wehrse and Peraiah (1979) attempted

to calculate lines in the rest frame of the star. In both cases, the maximum gas velocity employed was only 2 mean thermal units. The reason is that in the rest frame, the frequency-angle mesh should extend from $(-x-V_{\max})$ to $(x+V_{\max})$ where $x=(\nu-\nu_0)/\Delta_s$, Δ_s being some standard frequency interval. As the velocity $V_{\max}$ increases, this interval also increases and so does the number of frequency-angle points and the numerical operations. The excessive numerical operations introduce round-off errors and 'eat' into the real solution. Therefore, one has to restrict to small gas velocities.

However, in a comoving frame, the relative velocities do not exist and therefore we need not consider a large frequency-angle mesh. Mihalas, Kunasz and Hummer (1975, 1976) have solved the transfer equation in the comoving frame with both complete and partial frequency redistribution. However, their calculations are limited to show a comparison between the complete and partial redistribution.

In this paper, we present calculations of line formation in the comoving frame with partial redistribution in the framework of discrete space theory of radiative transfer. This is an extension of the calculations of lines in the comoving frame with complete redistribution (see Peraiah 1980) to partial frequency redistribution.

2. Solution of line transfer in the comoving frame with partial redistribution

We shall consider the radiative transfer equation in the comoving frame with a two-level atom approximation in non-LTE. The comoving terms are (see Mihalas, Kunasz and Hummer 1975)

$$\left\{(1-\mu^2)\,\frac{V(r)}{r}+\mu^2\frac{dV(r)}{dr}\right\}\frac{\partial I(x,\mu,r)}{\partial x}, \tag{1}$$

where $I(x, \mu, r)$ is the specific intensity of the ray with frequency $x=(\nu-\nu_0)/\Delta_s$, (Δ_s being some standard frequency interval and ν_0 is the central frequency of the line) making an angle $\cos^{-1}\mu$ with the radius vector at the radial point r. $V(r)$ is the radial velocity of the gas at r in mean thermal units. The radiative transfer equation in the comoving frame is written after including the terms in equation (1) (see Mihalas, Kunasz and Hummer 1975, 1976)

$$\mu\,\frac{\partial I(x,\mu,r)}{\partial r}+\frac{1-\mu^2}{r}\,\frac{\partial I(x,\mu,r)}{\partial \mu}=K(x,r)\,S_L(x,r)$$

$$+K_c(r)\,S_c(r)-[K(x,r)+K_c(r)]\,I(x,\mu,r)$$

$$+\left\{(1-\mu^2)\,\frac{V(r)}{r}+\mu^2\frac{dV(r)}{dr}\right\}\frac{\partial I(x,\mu,r)}{\partial x}, \tag{2}$$

and for the oppositely directed beam,

$$-\mu\,\frac{\partial I(x,-\mu,r)}{\partial r}-\frac{1-\mu^2}{r}\,\frac{\partial I(x,-\mu,r)}{\partial \mu}=K(x,r)\,S_L(x,r)$$

$$+ K_c(r)\, S_c(r) - [K(x, r) + K_c(r)]\, I(x, -\mu, r)$$

$$+ \left\{ (1-\mu^2)\, \frac{V(r)}{r} + \mu^2 \frac{dV(r)}{dr} \right\} \frac{\partial I(x, -\mu, r)}{\partial x} . \tag{3}$$

Here, $K_L(x, r)$ and $K_c(r)$ are the absorption coefficients per unit frequency interval in the line and continuum respectively. The quantities $S_L(x, r)$ and $S_C(r)$ are the line and continuum source functions respectively and are given by

$$S_L(x, r) = \frac{(1-\epsilon)}{\phi(x)} \int_{-\infty}^{+\infty} dx' \int_{-1}^{+1} R(x; x')\, I(x', \mu')\, d\mu' + \epsilon\, B(r), \tag{4}$$

and $$S_c(r) = \rho(r)\, B(r), \tag{5}$$

where $B(r)$ is the Planck function and $\rho(r)$ is model-dependent and is treated as an arbitrary function in this work. $K_L(x, r)$ is given by

$$K_L(x, r) = \phi(x) K_L(r), \tag{6}$$

and the profile function $\phi(x)$ is given by

$$\phi(x) = \int_{-\infty}^{+\infty} R(x, x')\, dx',$$

where $R(x, x')$ is the angle-averaged redistribution function (see Hummer 1962) given by

$$R_{I\text{-}A}(x, x') = \tfrac{1}{2}\, \mathrm{erfc}\,(|\bar{x}|), \tag{7}$$

where $$\mathrm{erfc}\,(|\bar{x}|) = \frac{1}{\sqrt{\pi}} \int_{|\bar{x}|}^{\infty} exp\,(-t^2)\, dt, \tag{8}$$

$\bar{x}$ being the maximum of $|x|$ and $|x'|$. The line profile is normalised so that,

$$\int_{-\infty}^{+\infty} \phi(x)\, dx = 1. \tag{9}$$

The quantity ϵ is the probability per scatter that a photon is lost by collisional de-excitation.

The integration of equations (2) and (3) is performed as described in Grant and Peraiah (1972) and Peraiah (1978, 1980). After discretisation equations (2) and (3) are written as,

$$\mathbf{M}\,[\mathbf{U}^{+}_{n+1} - \mathbf{U}^{-}_{n}] + \rho_c\,[\boldsymbol{\Lambda}^{+}\,\mathbf{U}^{+}_{n+1/2} + \boldsymbol{\Lambda}^{-}\,\mathbf{U}^{-}_{n+1/2}] + \tau_{n+1/2}\,\boldsymbol{\Phi}_{n+1/2}\,\mathbf{U}^{+}_{n+1/2}$$

$$= \tau_{n+1/2}\,\mathbf{S}_{n+1/2} + \tfrac{1}{2}(1-\epsilon)\,\tau_{n+1/2}\,\mathbf{R}_{n+1/2}\,\mathbf{W}_{n+1/2}\,[\mathbf{U}^{+}_{n+1/2} + \mathbf{U}^{-}_{n+1/2}]$$

$$+ \mathbf{M}_1\ \mathbf{d}\ \mathbf{U}^{+}_{n+1/2}, \tag{10}$$

and $\mathbf{M}\,[\mathbf{U}^{-}_{n} - \mathbf{U}^{-}_{n+1}] - \rho_c\,[\boldsymbol{\Lambda}^{+}\,\mathbf{U}^{-}_{n+1/2} + \boldsymbol{\Lambda}^{-}\,\mathbf{U}^{+}_{n+1/2}] + \tau_{n+1/2}\,\boldsymbol{\Phi}_{n+1/2}\,\mathbf{U}^{+}_{n+1/2}$

$$= \tau_{n+1/2}\,\mathbf{S}_{n+1/2} + \tfrac{1}{2}(1-\epsilon)\,\tau_{n+1/2}\,\mathbf{R}_{n+1/2}\,\mathbf{W}_{n+1/2}\,[\mathbf{U}^{+}_{n+1/2} + \mathbf{U}^{-}_{n+1/2}]$$

$$+ \mathbf{M}_1\ \mathbf{d}\ \mathbf{U}^{-}_{n+1/2} \tag{11}$$

$$\text{where } \mathbf{M} = \begin{bmatrix} \mathbf{M}_m & & & \\ & \mathbf{M}_m & & \\ & & \ddots & \\ & & & \mathbf{M}_m \end{bmatrix}, \quad \mathbf{M}_m = [\mu_j\,\delta_{jl}], \tag{12}$$

μs being the angle quadrature points.

$$\boldsymbol{\Lambda}^{\pm} = \begin{bmatrix} \boldsymbol{\Lambda}^{\pm}_m & & & \\ & \boldsymbol{\Lambda}^{\pm}_m & & \\ & & \ddots & \\ & & & \boldsymbol{\Lambda}^{\pm}_m \end{bmatrix}, \tag{13}$$

$\boldsymbol{\Lambda}^{\pm}_m$ are the curvature matrices (see Peraiah and Grant 1973). And,

$$\mathbf{U}^{\pm}_{n} = [\mathbf{U}^{\pm}_{1,n}\ ,\ \mathbf{U}^{\pm}_{2,n}\ ,\ \mathbf{U}^{\pm}_{3,n}, .., \mathbf{U}^{\pm}_{i,n}, .., \mathbf{U}^{\pm}_{I,n}]^{T}, \tag{14}$$

$$\mathbf{U}^{+}_{i,n} = 4\pi r^{2}_{n} \begin{bmatrix} I(\tau_n, +\mu_1, x_i) \\ I(\tau_n, +\mu_2, x_i) \\ \vdots \\ I(\tau_n, +\mu_J, x_i) \end{bmatrix}, \tag{15}$$

r_n being the radius of the nth shell and J and I are the total number of angles and frequency points. The subscript $n+\frac{1}{2}$ represents the average of the subscripted

parameter over the shell bounded by the radii r_n and r_{n+1}. The optical depth $\tau_{n+1/2}$ is defined as

$$\tau_{n+1/2} = K_L\,(r_{n+1/2})\,\Delta\, r, \tag{16}$$

$$\Delta r \quad = (r_{n+1} - r_n). \tag{17}$$

The quantity $\Phi_{n+1/2}$ is given by

$$\Phi_{n+1/2} = [\Phi_{kk'}]_{n+1/2} = (\beta + \phi_k)_{n+1/2}\,\delta_{kk'}\,, \tag{18}$$

$\beta = K_C \,/\, K_L$ and

$$k = j + (i-1)J;\ 1 \leqslant k \leqslant K = IJ, \tag{19}$$

$$\mathbf{S}_{n+1/2} = (\rho\beta + \epsilon\phi_k)_{n+1/2}\,B'_{n+1/2}, \tag{20}$$

$$\phi_k = \phi\,(x_i,\ \mu_j),$$

$$B'_{n+1/2} = 4\pi r^2_{n+1/2}\,B(r). \tag{21}$$

The quantity $R_{n+1/2}$ is the redistribution function. As we are considering the comoving frame, $R^{++} = R^{--} = R^{-+} = R^{+-} = R$, which corresponds to the redistribution function in static medium, $W_{n+1/2}$ is given by

$$W_k = a_i\,c_j,\ a_i = \frac{A_i\,R_{kk'}}{\Sigma\,R_{kk'}\,A_i\,C_j}\,, \tag{22}$$

where A's and C's are the weights of the frequency and angle quadratures respectively. The quantity ρ_c is the curvature factor given by

$$\rho_c = \Delta r/\bar{r}, \tag{23}$$

where $\bar{r}$ is the mean radius of the given shell. The last two terms in (10) and (11) represent the comoving terms given in (1) and

$$\mathbf{M}_1 = \mathbf{M}^1\,\Delta V_{n+1/2} + \mathbf{M}^2\,\rho_c\,V_{n+1/2}, \tag{24}$$

$$\left.\begin{aligned} \mathbf{M}^1 &= \begin{bmatrix} \mathbf{M}^1_m & & & \\ & \mathbf{M}^1_m & & \\ & & \ddots & \\ & & & \mathbf{M}^1_m \end{bmatrix},\quad \mathbf{M}^1_m = [\mu_j^2\,\delta_{jl}] \\ \mathbf{M}^2 &= \begin{bmatrix} \mathbf{M}^2_m & & & \\ & \mathbf{M}^2_m & & \\ & & \ddots & \\ & & & \mathbf{M}^2_m \end{bmatrix},\quad \mathbf{M}^2_m = [1-\mu_j^2]\,\delta_{jl} \end{aligned}\right\}\ j, l = 1, \ldots, J. \tag{25}$$

$V_{n+1/2}$ is the average velocity in the shell bounded by radii r_n and r_{n+1} and $\Delta V_{n+1/2}$ is given by

$$\Delta V_{n+1/2} = V_{n+1} - V_n. \tag{26}$$

The matrix **d** represents the frequency derivative and its form is determined from the condition of flux conservation in a purely scattering medium (see Peraiah 1980). This is given by

$$\mathbf{d} = \begin{bmatrix} -d_1 & d_1 & & & & \\ -d_2 & 0 & d_2 & & & \\ & -d_3 & 0 & d_3 & & \\ & & \cdot & \cdot & \cdot & \\ & & & \cdot & \cdot & d_{I-1} \\ & & & & -d_I & d_I \end{bmatrix} \tag{27}$$

where $d_i = (X_{i+1} - X_{i-1})^{-1}$ for $i = 2, 3, \ldots I-1$ and we put

$$d_1 = d_I = 0. \tag{28}$$

By applying the diamond scheme to replace the average intensities $\mathbf{u}^{\pm}_{n+1/2}$ in equations (10) and (11) and arranging the resulting equations in the form of the 'interaction principle' we obtain the reflection and transmission operators(see Appendix). Calculation of the diffuse radiation field in the line in the comoving frame can be done as described in Grant and Hunt (1969).

3. Results and discussion

The calculations in a comoving frame can be easily made as the redistribution function does not change when the gas moves unlike that in the rest frame wherein the change in the redistribution function should be taken into account at every radial point in the moving gas (see Peraiah 1978). However, the radiation field obtained in the comoving frame should be translated into either (i) the rest frame of the star which describes the solution of radiative transfer in spherical symmetry or (ii) onto the frame of reference of the observer at infinity. In this paper, we have performed the latter type of calculations as these may be useful for direct

comparison with observations. In Fig. 1, we have described how the radiation field in the comoving frame has been translated into the frame of reference of the observer at the earth. The procedure is briefly as follows: We solve the radiative transfer equation (see Peraiah 1980) in the comoving frame (see equations (2) and (3)) by assuming a velocity distribution given by

$$V(r) = V_A + \frac{V_B - V_A}{B - A}\,(r - A), \tag{29}$$

where $V(r)$ is the velocity of the gas at the radial point r and V_A and V_B and the velocities at the inner and outer radii A and B of the atmosphere respectively. All velocities are measured in mean thermal unit and we have considered the density varying as

$$\rho(r) \sim 1/[r^2 V(r)], \tag{30}$$

so that the optical depth varies as $1/r$. When the solution of transfer is obtained, we can calculate the frequency and angle-independent source functions $S(r)$ at every radial point by the relation

$$S_n = \sum_{i=1}^{I} A_i \sum_{j=1}^{J} S(x_i, \mu_j, \tau_n)\, C_j. \tag{31}$$

The optical depth is calculated along the parallel rays as shown in Fig. 1 and not along the radial direction in the atmosphere. With the help of equations (29), (30) and (31) we can calculate the fluxes received at infinity. We have selected

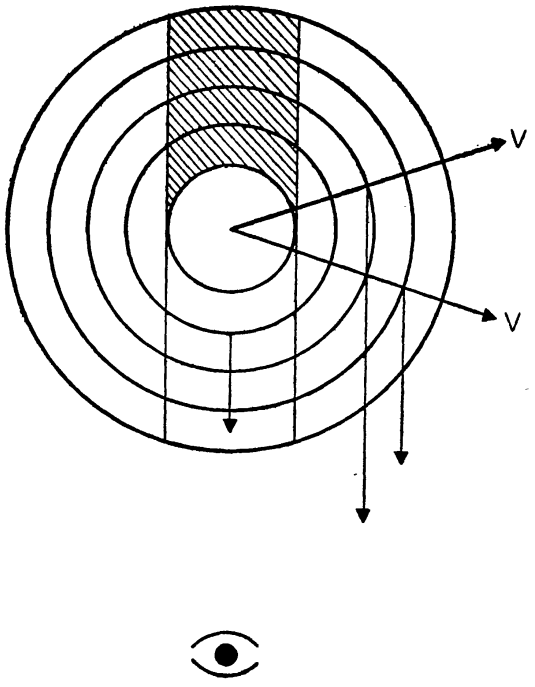

Figure 1. Diagram to show how fluxes are calculated at infinity.

a few representative values of the parameters ϵ, β, V_A, V_B, B/A. The total optical depth has been taken to be $\approx 10^3$ at the line centre. For boundary conditions see Peraiah (1978, 1980).

The results are presented in Figs 2 to 9. In Figs 2–5, we give the frequency and angle-integrated source functions for the parameters shown in the figures. In Fig. 2, the source functions are given for $B/A = 3$, and $\epsilon = \beta = 0$ and $V_B = 0$, 10 and 30. We notice that the source function is reduced by nearly 4 orders of magnitude at the boundary in the static case, whereas in the case of moving gas it is further reduced to 5 orders of magnitude.

Similar effects have been found when the ratio of outer to inner radii B/A is increased to 9. In this case the source function is reduced by 7 orders of magnitude when the velocity reaches 30 at the surface (see Fig. 3). The radiation field is diluted over an extended medium and this effect is further accentuated when the gases in the atmosphere move radially outwards. In Figs 4 and 5, we present the frequency and angle-independent source functions corresponding to the parameters $\epsilon = 10^{-3}$, $\beta = 0$ and $B/A = 3$ and 9. The same effects are found in general as for a purely scattering medium ($\epsilon = 0, \beta = 0$). However, the sharp rise in the source function at τ_{max} is due to the nature of the boundary condition we have given *i.e.* no

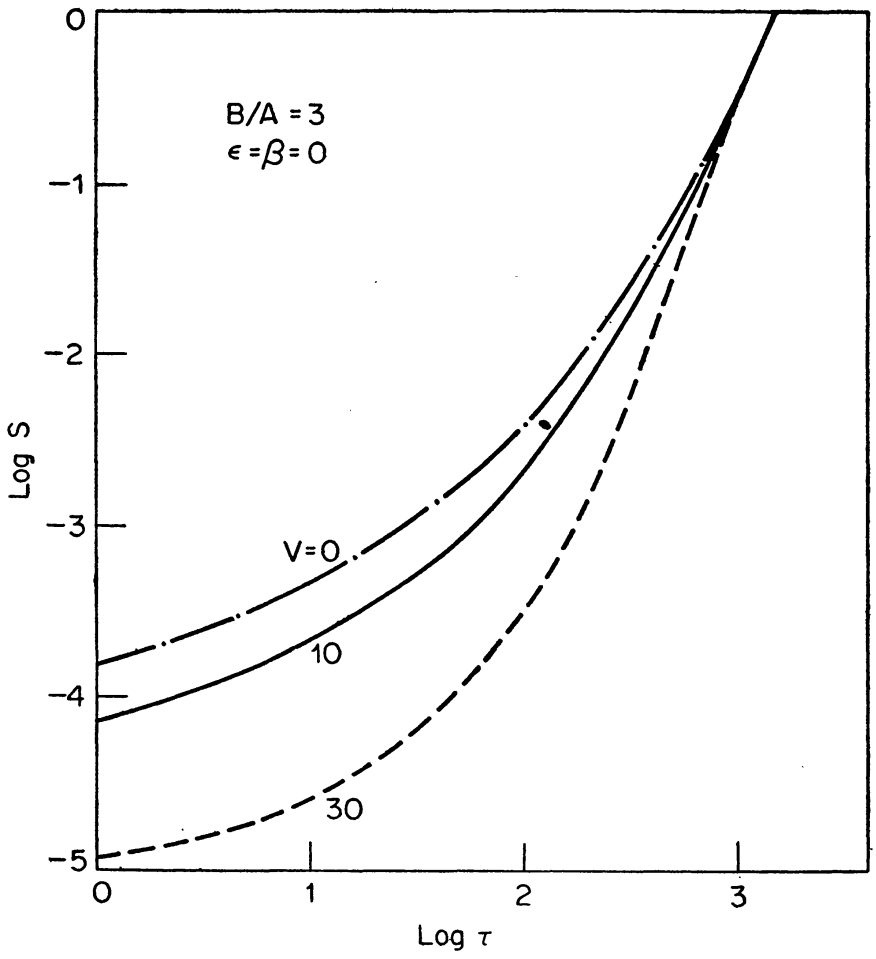

Figure 2. Frequency and angle independant source functions for $B/A=3$, $\epsilon=\beta=0$.

radiation is incident at $\tau = \tau_{max}$. In the vicinity of τ_{max}, in the atmosphere, the source function reaches a maximum as there is line emission ($\epsilon = 10^{-3}$). We present the flux profiles received by the observer at the earth in Figs 6–9. We have plotted F_x ($=F(x)/F(x_{max})$) versus Q ($= x/x_{max}$). The profiles given in Figs 6 and 7 correspond to the source functions given in Figs 2 and 3 and the profiles given in (8) and (9) correspond to the source functions given in Figs 4 and 5. We notice absorption lines in the case of purely scattering medium as seen from Figs 6 and 9. When the velocities increase their line centres are shifted towards the blue side (see Figs 6 and 7). In Figs 8 and 9 the flux profiles for line emission are presented. In a static medium, we obtain an emission line with central absorption. However, when motion is introduced, we notice an emission line with reduced widths. These profiles are quite similar to those observed in some of the quasars, see for example Baldwin (1975) and Baldwin and Netzer (1978).

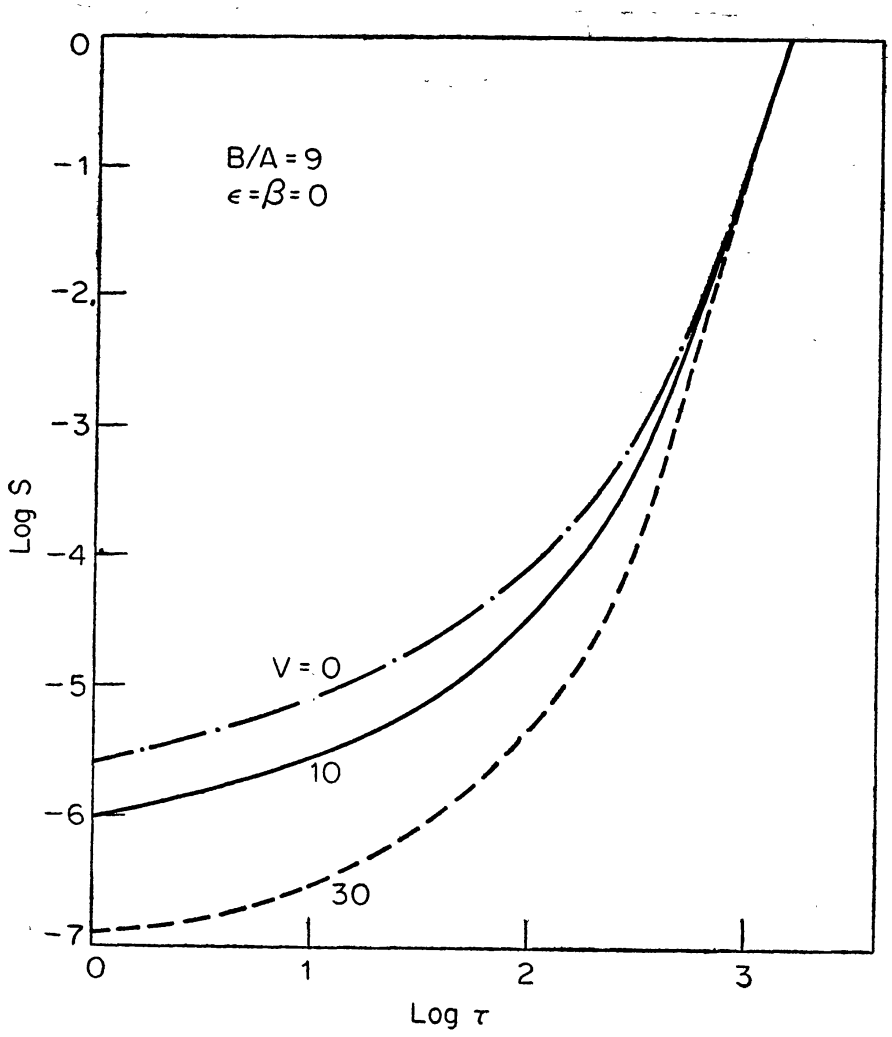

Figure 3. Same as in Fig. 2 with $B/A=9$.

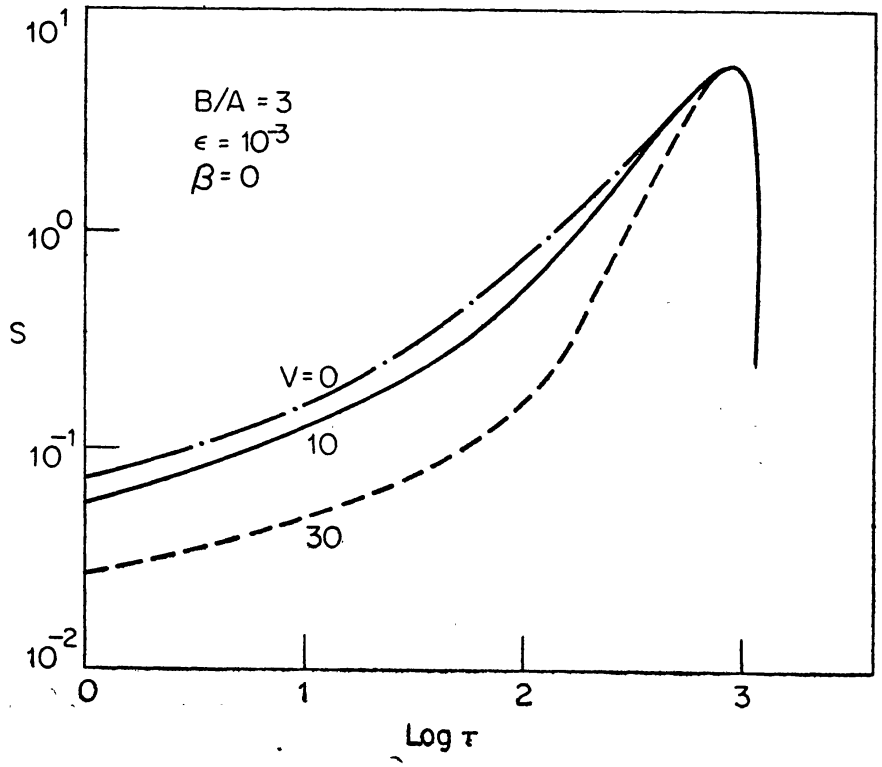

Figure 4. Same as in Fig. 2 with $\epsilon=10^{-3}$.

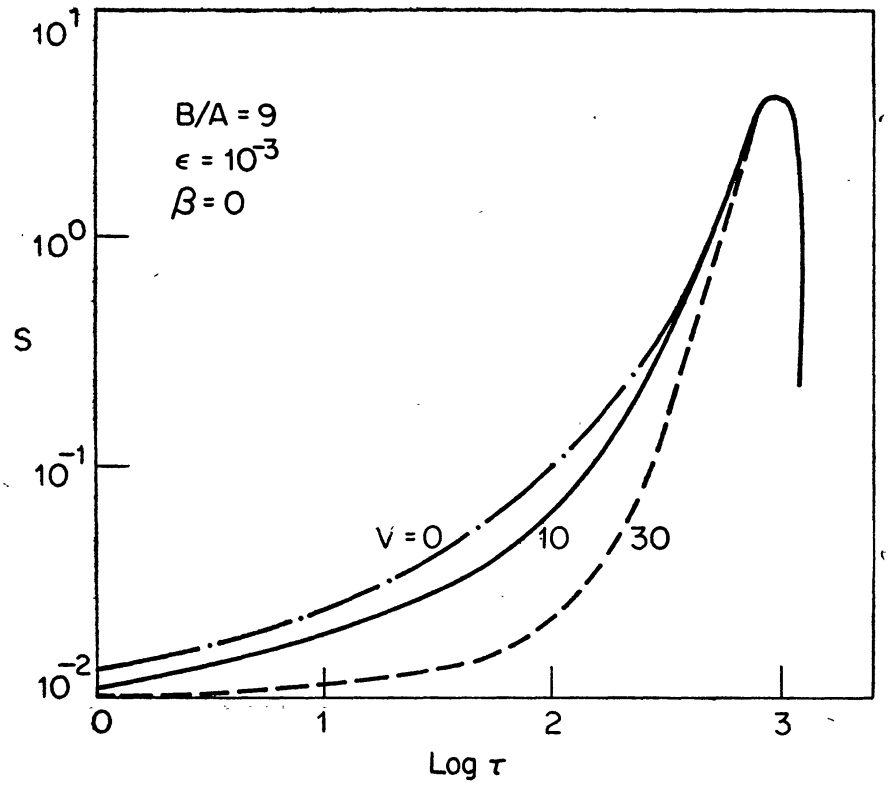

Figure 5. Same as in Fig. 2 with $B/A=9$ and $\epsilon=10^{-3}$.

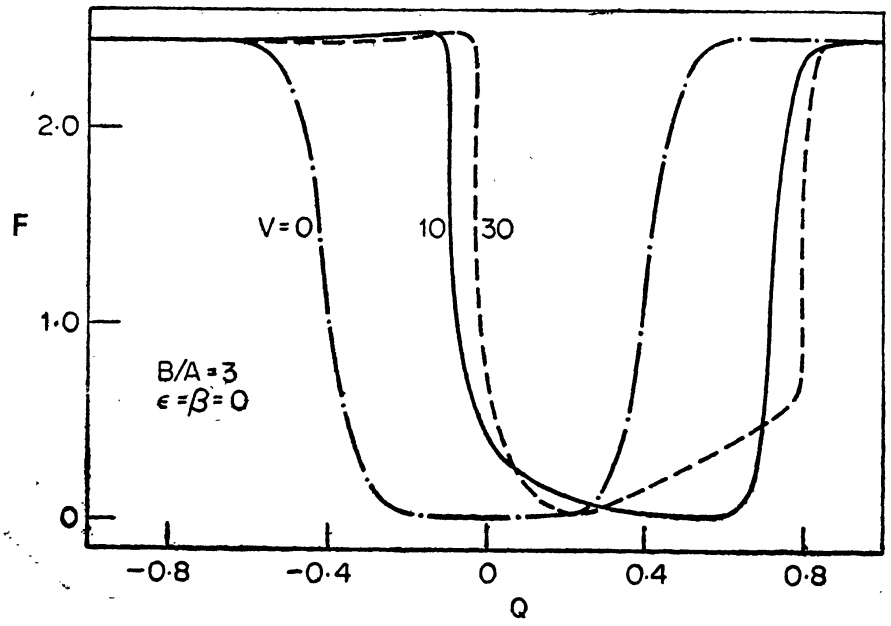

Figure 6. Flux profiles of the lines received at the observer $F = F(x)/F(x_{max})$ and $Q = x/x_{max}$ corresponding to the source functions given in Fig. 2.

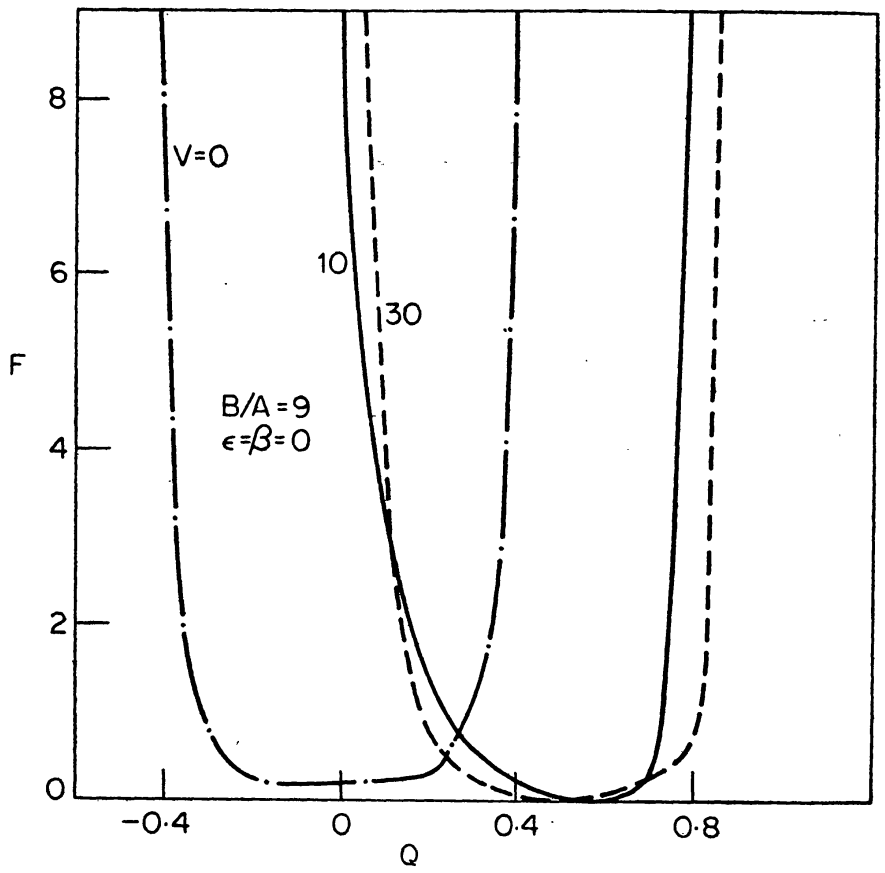

Figure 7. Flux profiles corresponding to the source functions given in Fig. 3.

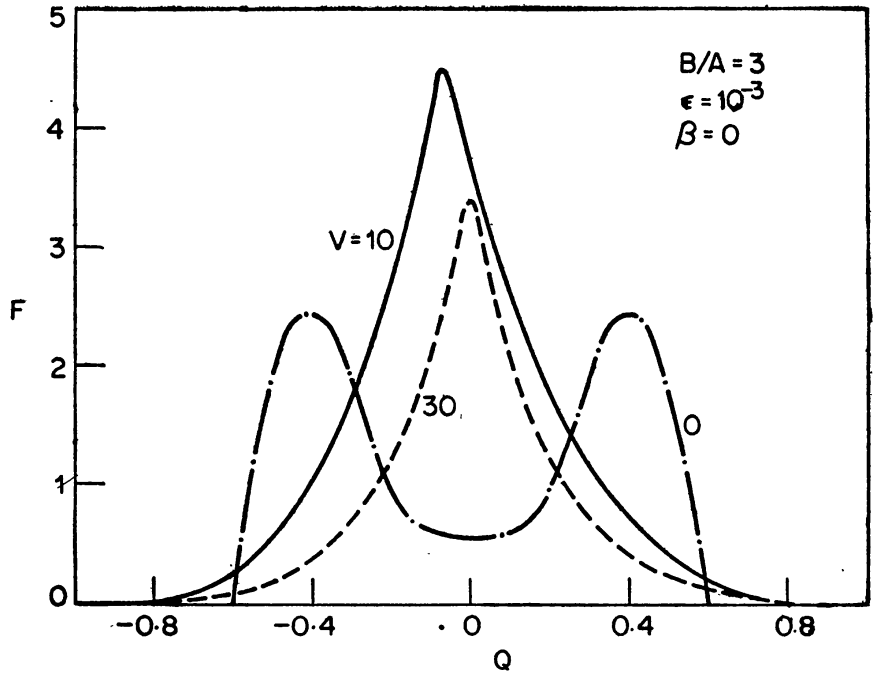

Figure 8. Same as in Fig. 6 but corresponding to the source functions of Fig. 4.

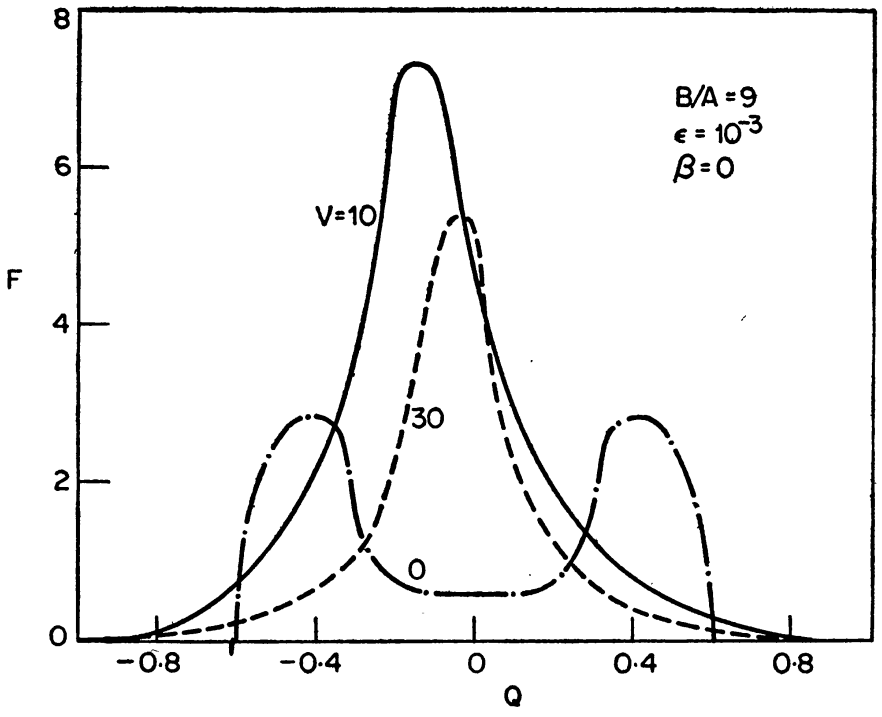

Figure 9. Same as in Fig. 6 corresponding to the source functions given in Fig. 5.

4. Conclusions

Comoving frame calculations have been performed by using the angle-averaged partial frequency redistribution function R_I to obtain flux profiles which can be compared with observations. The profiles calculated with line emission ($\epsilon = 10^{-8}$) resemble those observed in some of the quasars.

Appendix

The transmission and reflection matrices in the basic ' cell ' are,

$$\mathbf{t}(n+1, n) = \mathbf{G}^{+-}[\Delta^{+}\mathbf{A}_{+} + \mathbf{g}^{+-}\mathbf{g}^{-+}],$$

$$\mathbf{r}(n+1, n) = \mathbf{G}^{-+}\mathbf{g}^{-+}[\mathbf{I} + \Delta^{+}\mathbf{A}_{+}),$$

and the source vector is

$$\sum^{+} = \mathbf{G}^{+-}[\Delta^{+} + \mathbf{g}^{+-}\Delta^{-}]\,\mathbf{S}\,\tau.$$

Similarly $\mathbf{t}(n, n+1)$, $\mathbf{r}(n, n+1)$ and Σ^{-} can be written by interchanging the subscripts and superscripts, namely the + and − signs ($\mathbf{I}$ is unit matrix). Also,

$$\mathbf{G}^{+-} = [\mathbf{I} - \mathbf{g}^{+-}\mathbf{g}^{-+}]^{-1},\ \mathbf{g}^{+-} = \tfrac{1}{2}\tau\,\Delta^{+}\mathbf{Y}_{-}$$

$$\Delta^{+} = [\mathbf{M} + \tfrac{1}{2}\tau\,\mathbf{Z}_{+}]^{-1},\ \mathbf{Z}_{+} = \Phi - \tfrac{1}{2}\sigma\,\mathbf{R}\,\mathbf{W} + \frac{\rho_c\,\Lambda^{+}}{\tau} - \frac{\mathbf{M}_1\mathbf{d}}{\tau}$$

$$\mathbf{Z}_{-} = \Phi - \tfrac{1}{2}\sigma\mathbf{R}\mathbf{W} - \frac{\rho_c\Lambda^{+}}{\tau} - \frac{\mathbf{M}_1\mathbf{d}}{\tau}$$

$$\mathbf{Y}_{+} = \tfrac{1}{2}\sigma\,\mathbf{R}\,\mathbf{W} + \frac{\rho_c\,\Lambda^{-}}{\tau},\ \mathbf{Y}_{-} = \tfrac{1}{2}\sigma\,\mathbf{R}\,\mathbf{W} - \frac{\rho_c\,\Lambda^{-}}{\tau}$$

$$\mathbf{A}_{+} = \mathbf{M} - \tfrac{1}{2}\tau\,\mathbf{Z}_{+},\ \mathbf{A}_{-} = \mathbf{M} - \tfrac{1}{2}\tau\,\mathbf{Z}_{-}.$$

Similarly $\mathbf{G}^{-+}$, $\mathbf{g}^{-+}$, Δ^{-}, are written by interchanging the subscripts and superscripts + and − signs. And $\sigma = 1 - \epsilon$.

References

Baldwin, J. A. 1975, *Astrophys. J.*, **201**, 26.
Baldwin, J. A., Netzer, H. 1978, *Astrophys. J.*, **226**, 1.
Grant, I. P., Hunt, G. E. 1969, *Proc. R. Soc. London Ser. A*, **313**, 183.
Grant, I. P., Peraiah, A. 1972, *Mon. Not. R. astr. Soc.*, **160**, 239.
Hummer, D. G. 1962, *Mon. Not. R. astr. Soc.*, **125**, 21.
Hummer, D. G., Kunasz, P. B. 1974, *Mon. Not. R. astr. Soc.*, **166**, 19.

Mihalas, D., Kunasz, P. B., Hummer, D. G. 1975, *Astrophys. J.*, **202,** 465.
Mihalas, D., Kunasz, P. B., Hummer, D. G. 1976, *Astrophys. J.*, **210,** 419.
Peraiah, A. 1978, *Kodaikanal Obs. Bull. Ser. A*, **2,** 115.
Peraiah, A. 1980, *Acta Astr.* (in press)
Peraiah, A., Grant, I. P. 1973, *J. Inst. Math. Its Appl.*, **12,** 75.
Peraiah, A., Wehrse, R. 1978, *Astr. Astrophys.*, **70,** 213.
Wehrse, R., Peraiah, A. 1979, *Astr. Astrophys.*, **71,** 289.